



Effect of Loading Sequence in Compressive Fatigue of Concrete: Experimental and Theoretical Evidence

Abedulgader Baktheer^(✉) , Josef Hegger , and Rostislav Chudoba 

Institute of Structural Concrete, RWTH Aachen University, Aachen, Germany
Abaktheer@imb.rwth-aachen.de

Abstract. A realistic prediction of the fatigue life of concrete under high-cycle loading scenarios with variable amplitudes is of utmost importance for a reliable and economically efficient design of structural infrastructures for transportation and energy supply. Current design codes estimate fatigue life under variable amplitudes using the Palmgren-Miner rule, which assumes a linear scaling between the lives measured for uniform cyclic loading scenarios. However, several series of experiments conducted in the past showed that this assumption is not valid and may lead to unsafe design. The paper shows recent results of experimental campaign focused on the compressive fatigue behavior of concrete in response to a subcritical cyclic loading with variable amplitudes. The obtained results present evidence of the effect of loading sequence on the fatigue life of concrete. To substantiate the experimental results, an interpretation of the phenomenology behind the sequence effect is provided in terms of the dissipated energy due to damage within the material structure.

Keywords: Concrete fatigue · Cyclic loading · Loading sequence effect · Variable amplitudes · Damage accumulation · Energy dissipation

1 Introduction

In modern high-performance RC structures, the compressive fatigue behavior of concrete is becoming crucial due to the high material utilization [1]. This is especially important in prestressed slender structures such as concrete wind turbine towers, where cyclic loading leads to stress fluctuations around very high permanent compressive stresses. The fatigue behavior of concrete has been studied mainly experimentally at constant amplitudes in the last decades, e.g. [2–4]. Based on these studies, the fatigue life of concrete is typically characterized using Wöhler/S-N curves. However, in reality, concrete members and structures are subjected to complex loading scenarios with variable amplitude, such as stochastic wind action in offshore and offshore wind farms [5].

In spite of the fact that the effect of loading sequence is of significant importance for any structure subjected to fatigue loading, so far little experimental research has been reported in the literature to investigate the effect of loading sequence on the fatigue behavior of concrete. An experimental program conducted by Holmen [6] used a loading

scenario consisting of two cyclic loading ranges, i.e., high (H) and low (L) with different sequences (H-L and L-H). The obtained results were compared with the concept of P-M rule. Obviously, the failure for the (H-L) scenario was observed much earlier than predicted by the P-M rule. The experimental results presented by Petkovic et al. [7] show that the P-M rule provides a conservative prediction of fatigue life for the specimens tested with the (L-H) scenario. Moreover, a reverse sequence effect reported in the literature for bending fatigue of concrete e.g. [8–10].

Current design codes, e.g. [11, 12] estimate the fatigue life under variable amplitudes using the Palmgren-Miner (P-M) rule [13, 14], which assumes a linear scaling between lifetimes measured for uniform cyclic loading scenarios. The few available experimental series conducted in the past, however, indicate that this assumption is not valid and that it may lead to unsafe design. To provide evidence of the effect of loading sequence on the fatigue life, this effect has been investigated comprehensively in the test program presented in the current contribution. Furthermore, the phenomenology behind the fatigue sequence effect has been theoretically interpreted using an energetic concept.

2 Experimental Program

2.1 Material Properties, Test Program and Data Recording

Compressive tests have been performed using cylinder test specimens with a diameter of 150 mm and a height of 300 mm (Fig. 1). The test program consists of 57 cylinder specimens. According to FIB Model Code 2010 [11] the concrete used in the study is classified into concrete strength classes C40/50. A W/C ratio of 0.5 was used for the concrete mixture with the cement type (CEM II 42.5 N). The aggregate composition consists of 62% limestone and 38% quartz sand with a maximum grain size of 8 mm. The specimens were produced and tested within one batch to guarantee the consistency and comparability of the material properties. The performed test campaign is summarized in Table 1 showing the correspondence between the applied loading scenarios (LS1–LS3) and the performed replications of a particular test configuration.

The monotonic as well as the cyclic tests were carried out in a testing machine with a hydropuls actuator. Although the cylinders were polished, the load was introduced with the help of a flexible calotte. During the experiments the machine load and the strains of the concrete cylinders were measured continuously using linear variable differential

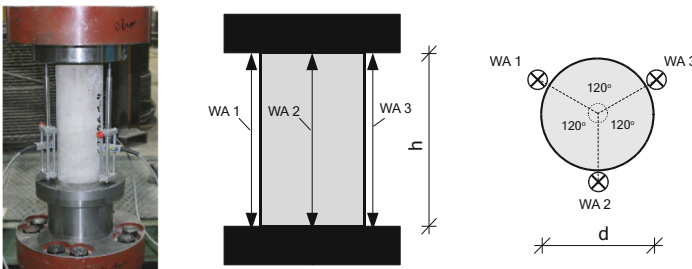


Fig. 1. Cylinder specimen geometry with 3 LVDTs positioned around the perimeter.

transformers (LVDTs). Three LVDTs were placed between the steel support plates and distributed equally every 120° (Fig. 1). Further details of the test program can be found in [15].

2.2 Loading Scenarios

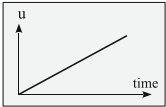

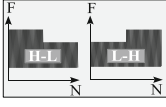
To study the effect of loading sequence on the concrete fatigue behavior, three loading scenarios are considered in this study.

LS1: The first loading scenario introduces a monotonically increasing control displacement with the rate of 1.0 mm/min. This test delivers the ultimate compression load F_u .

LS2: The second loading scenario represents the standard fatigue loading with constant amplitudes. The load has been applied with a frequency of 5 Hz. The upper load levels have been varied between $S^{\max} = 0.65$ to $S^{\max} = 0.75$, and lower load level was set to $S^{\min} = 0.05$. The purpose of this scenario is to study the concrete fatigue behavior under constant amplitudes and to determine the fatigue life for the studied loading ranges.

LS3: The third scenario is a fatigue loading with two different levels applied in sequence i.e. high–low (H–L) and low–high (L–H). In these loading scenarios first load level e.g. the high for (H–L) sequence is applied with a specific number of cycles, then the second load level is applied until fatigue failure. The load has been applied with a frequency of 5 Hz. The upper load levels were similar to LS2. This loading scenario is the typical scenario to investigate the sequence effect on the fatigue life.

Table 1. Description of the loading scenarios used in the experimental program.

Loading scenario	Description	Figure	Number of tests
LS1	Monotonic loading		9
LS2	Fatigue loading with constant amplitudes		24
LS3	Fatigue loading with two loading ranges and different sequence		24

3 Experimental Results and Discussion

3.1 Monotonic and Fatigue Behavior

The average compressive strength of the tested 9 concrete cylinder specimens under monotonic loading (LS1) was 61.55 MPa with a coefficient of variation (CoV) scatter of 3.79%. The average of elastic modulus was 31900 MPa.

The fatigue behavior of the tested concrete has been characterized in terms of fatigue creep curves and Wöhler curves as shown in Fig. 2. The fatigue creep curves under constant amplitudes for representative tests are plotted in Fig. 2a, b. The typical shape of fatigue creep curves, i.e. the rapid increase of the strain in the first and last stages and nearly linear growth in the middle stage is reproduced in all tests. By comparing Fig. 2a and Fig. 2b, we can conclude that the range of strain growth between the first and last cycle decreases with an increasing the load level.

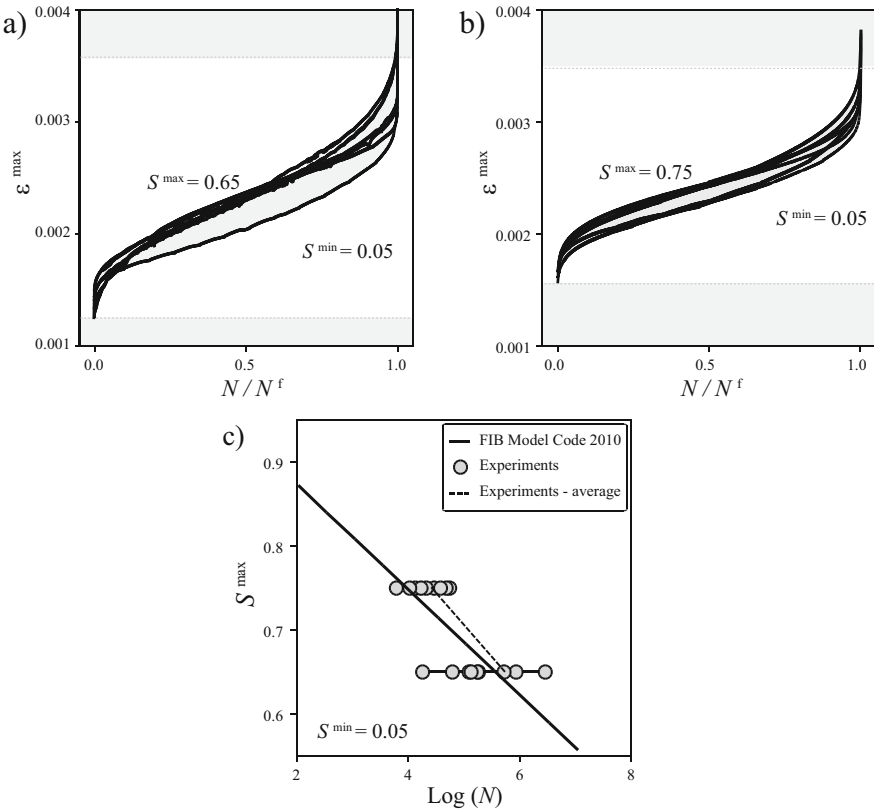


Fig. 2. Fatigue response under constant amplitudes loading scenario (LS2): a, b) fatigue creep curves for; c) Wöhler curve.

The number of cycles to fatigue failure for varied upper load levels S_{\max} measured in the performed tests is summarized in Fig. 2c. The numerical values for the investigated

load levels including the average, minimum and maximum values of the number of cycles to fatigue failure can be found in [15]. The obtained results show longer fatigue life than predicted by the Wöhler curve proposed by the fib Model Code 2010 [11]. However, for a relevant comparison more tests would be necessary. Still, for the investigation of the loading sequence effect such a number of specimens is reasonable to determine the fatigue life of the individual loading ranges.

3.2 Sequence Effect Using Two Loading Ranges

The effect of loading sequence was investigated using a loading scenario consisting of two loading ranges with the upper load levels (H) and (L). Each loading range applied separately would lead to failure after N_H^f and N_L^f loading cycles. The question is what number of loading cycles leads to fatigue failure when the two loading ranges are combined in a sequence, either (H–L) or (L–H). The obtained experimental results are plotted in Fig. 3a–c.

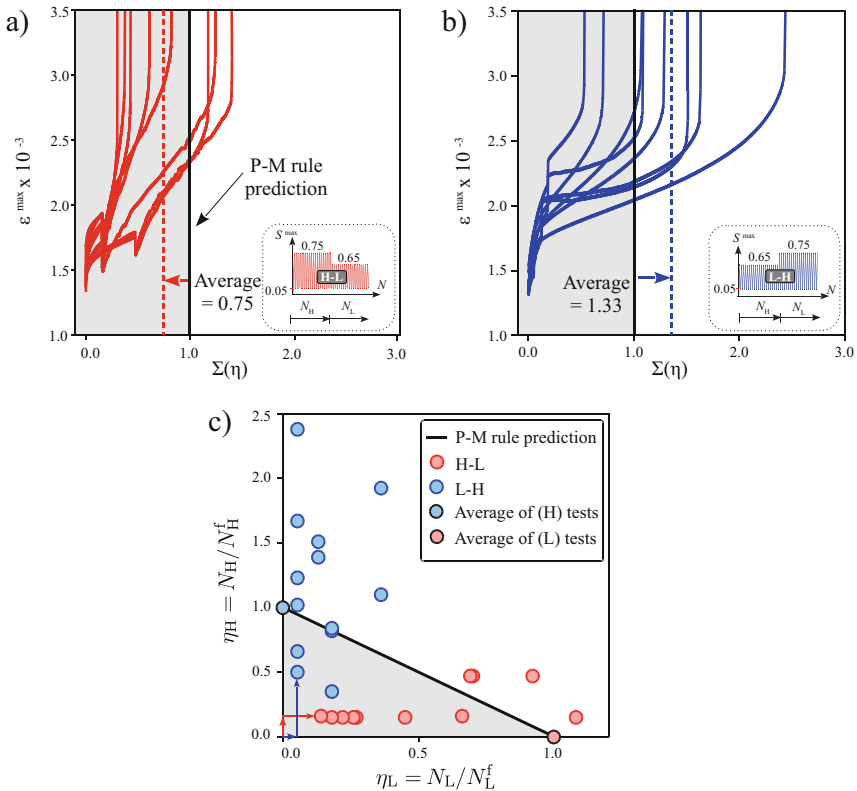


Fig. 3. Load sequence effect in concrete fatigue: a, b) fatigue creep curves for (H–L) and (L–H) loading scenario respectively; c) comparison with the predicted fatigue life of P–M rule.

The test results are visualized in relation to the Palmgren–Miner (P–M) rule providing a baseline for the evaluation of the sequence effect. The fatigue creep curves obtained for the (H–L) and (L–H) loading scenarios are depicted in Fig. 3a, b. The lifetime on the horizontal axis is normalized with respect to the lifetime prediction by the P–M rule assuming the fatigue failure once the sum of the consumed fatigue life $\sum \eta$ of both (H) and (L) is equal to 1. Even though the results show a considerable scatter, an obvious trend can be observed. The average of the consumed fatigue life $\sum \eta$ is less than 1.0 for the (H–L) sequence as depicted in Fig. 3a, and larger than 1.0 for the (L–H) sequence as depicted in Fig. 3b. This indicates an unsafe prediction of the P–M rule for (H–L) scenario and conservative prediction of (L–H) scenario. These results confirm the observation presented in [6].

4 Theoretical Interpretation of the Loading Sequence Effect

The summarized experimental data in Fig. 3 indicate that the (H–L) scenario accelerates the fatigue failure with respect to the P–M linear scaling, while (L–H) scenario slows it down. Obviously, the kind of a loading sequence has a significant influence on the concrete fatigue life. The theoretical explanation of the sequence effect can be provided based on the qualitative profiles of energy dissipation due to damage during the fatigue life. Assuming that energy is dissipated uniformly within the volume of the cylindrical test specimen during subcritical compressive cyclic loading the superposition of energy dissipation profiles along the lifetime measured for constant amplitudes becomes possible and can explain the experimentally observed misfit with respect to the P–M rule.

Consider the two curves in Fig. 4 showing the history of energy dissipation for the uniform cyclic loading (H) and (L) and for their ordered combinations (H–L) and (L–H). The energy dissipation profile for load (H) is assumed to be higher than for (L) with almost the equal accumulated energy dissipation at fatigue failure, which is in agreement with the numerical results presented in [16] using the recently developed microplane fatigue model [17, 18]. These numerical results also show that the energy dissipated due to the damage is approximately the same for both loading ranges (H) and (L). The left figure (Fig. 4a) outlines a postulate that when the cyclic load changes from the higher level (H) to the lower level (L), the further dissipation profile of the (H–L) scenario can be predicted by switching to the branch observed for the uniform scenario (L). The switching is performed at the level of energy dissipation ζ_H reached at the end of the first loading range (H). In other words, the continuation point on branch η_L is associated with the same amount of dissipated energy, i.e. $\zeta_L = \zeta_H$ (for further explanation see [15]). With the present superposition rule, we might now define complex loading scenarios and directly predict a combined fatigue life, e.g. for (H–L), (L–H) or even more complex loading histories.

The energy based superposition provides a transparent explanation of the sequence effect observed in the performed test series. An (H–L) scenario depicted in Fig. 4a must necessarily lead to the reduction of the fatigue life compared to the P–M rule. On the other hand, an L–H scenario shown in Fig. 4b results in a longer lifetime compared to the P–M superposition rule. It must be stressed, however, that the described explanation of

the sequence effect is not valid for problems with macroscopic stress redistribution and strain localization within the volume of a specimen, e.g. propagation of tensile cracks in the bending test or debonding in the pull-out.

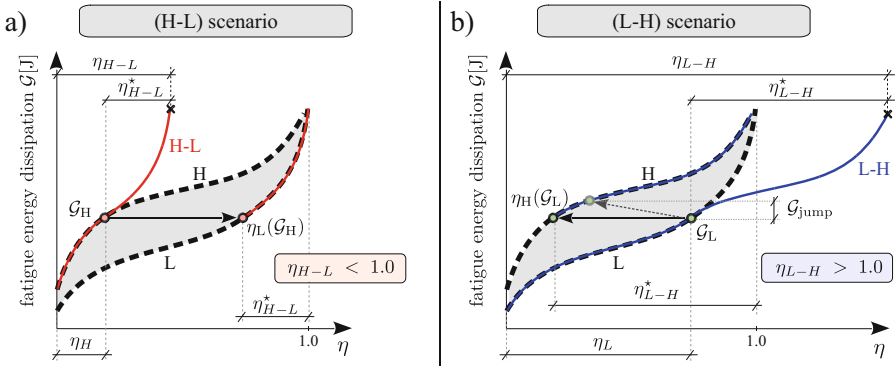


Fig. 4. Qualitative evolution of energy dissipation during fatigue life explaining the load sequence effect observed in compressive fatigue loading of concrete: a) (H–L) scenario; b) (L–H) scenario.

5 Conclusions and Outlook

The load sequence effect observed in the few available experimental studies in the literature indicating that the well-known P–M rule does not realistically predict the fatigue life under variable amplitudes has been confirmed by the present experimental study. The test results reveal unsafe prediction by the P–M rule for (H–L) load sequence and a conservative prediction for the (L–H) load sequence. To substantiate the experimentally observed sequence effect during compression, a theoretical analysis of the evolution of energy dissipation during fatigue loading has been performed.

The proposed energy-based explanation of the sequence effect shows the potential for further development of models that can realistically predict the fatigue life of concrete structures under generally variable fatigue loading scenarios. Furthermore, advanced and physically based fatigue models for concrete fatigue can be used for further investigation of the fatigue behavior of concrete under a wide range of complex loading scenarios based on measured data, which in the long run can lead to the derivation of improved design rules for predicting the fatigue life of fatigue-relevant structures such as wind power plants.

Acknowledgements. The work was supported by the Federal Ministry for Economic Affairs and Energy, Germany (BMWi), in the framework of the joint project (WinConFat), (Project No: 0324016C), and by the Deutsche Forschungsgemeinschaft (DFG, German Research Foundation), in the scope of the joint Project (CumFatiCon), (Project No. 412131890). This support is gratefully acknowledged.

References

1. Schmidt B, Schneider S, Marx S (2019) Concrete fatigue-safety and development potential of current design concepts. *Bautechnik* 96:329–337
2. Kim J-K, Kim Y-Y (1996) Experimental study of the fatigue behavior of high strength concrete. *Cem Concr Res* 26:1513–1523. [https://doi.org/10.1016/0008-8846\(96\)00151-2](https://doi.org/10.1016/0008-8846(96)00151-2)
3. Schneider S, Humme J, Marx S, Lohaus L (2018) Untersuchungen zum Einfluss der Probekörpergröße auf den Ermüdungswiderstand von hochfestem Beton. *Beton und Stahlbetonbau* 113:58–67. <https://doi.org/10.1002/best.201700051>
4. Song Z, Konietzky H, Cai X (2021) Modulus degradation of concrete exposed to compressive fatigue loading: Insights from lab testing. *Struct Eng Mech* 78(3):281–296
5. Lenschow R (1980) Long term random dynamic loading of concrete structures. *Materiaux et Construction* 13:274–278. <https://doi.org/10.1007/BF02474050>
6. Holmen JO (1982) Fatigue of concrete by constant and variable amplitude loading. *ACI Symp Publ* 75:71–110
7. Petkovic G, Lenschow R, Stemland H, Rosseland S (1990) Fatigue of high-strength concrete. *Spec Pub* 121:505–526. <https://doi.org/10.14359/3740>
8. Hilsdorf HK, Kesler CE (1966) Fatigue strength of concrete under varying flexural stresses. *J Proc* 63:1059–1076. <https://doi.org/10.14359/7662>
9. Baktheer A, Becks H (2021) Fracture mechanics based interpretation of the load sequence effect in the flexural fatigue behavior of concrete using digital image correlation. *Constr Build Mater* 307:124817. <https://doi.org/10.1016/j.conbuildmat.2021.124817>
10. Baktheer A, Camps B, Hegger J, Chudoba R (2018) Numerical and experimental investigations of concrete fatigue behaviour exposed to varying loading ranges. In: *The 5th fib congress*. Melbourne, pp 1110–1123. ISBN: 978-1-877040-15-3
11. fib Model Code (2010) International Federation for Structural Concrete, fib model code for concrete structures. <https://doi.org/10.1002/9783433604090>
12. EN-1992-2. 2005. Eurocode 2: Design of concrete structures, Part 2: Concrete bridges - Design and detailing rules. European Committee for Standardisation
13. Palmgren A (1924) Die Lebensdauer von Kugellagern (Durability of ball bearings). *Zeitschrift des Vereines Deutscher Ingenieure (VDI Zeitschrift)* 68:339–341
14. Miner MA (1945) Cumulative damage in fatigue. *J Appl Mech* 12(3):159–164
15. Baktheer A, Chudoba R (2021) Experimental and theoretical evidence for the load sequence effect in the compressive fatigue behavior of concrete. *Mater Struct* 54(2):1–23. <https://doi.org/10.1617/s11527-021-01667-0>
16. Aguilar M, Baktheer A, Chudoba R (2021) Numerical investigation of load sequence effect and energy dissipation in concrete due to compressive fatigue loading using the new microplane fatigue model MS1. In: Onate E, Peric D, Chiumenti M, de Souza Neto E (eds) *COMPLAS 2021*, Barcelona, Spain. <https://doi.org/10.23967/complas.2021.053>
17. Baktheer A, Aguilar M, Hegger J, Chudoba R (2019) Microplane damage plastic model for plain concrete subjected to compressive fatigue loading. In: *10th International conference on fracture mechanics of concrete and concrete structures, FraMCoS-X*. <https://doi.org/10.21012/FC10.233196>
18. Baktheer A, Aguilar M, Chudoba R (2021) Microplane fatigue model MS1 for plain concrete under compression with damage evolution driven by cumulative inelastic shear strain. *Int J Plast* 143:102950. <https://doi.org/10.1016/j.ijplas.2021.102950>